Experimental observation of transient $\delta^{18}O$ interaction between snow and advective airflow under various temperature gradient conditions

Pirmin Philipp Ebner[1], Hans Christian Steen-Larsen[2, 3], Barbara Stenni[4], Martin Schneebeli[1,*], and Aldo Steinfeld[5]

[1] *WSL Institute for Snow and Avalanche Research SLF, 7260 Davos Dorf, Switzerland*

[2] *LSCE Laboratoire des Sciences du Climat et de l'Environnement, Gif-Sur-Yvette Cedex, France*

[3] *Center for Ice and Climate, Niels Bohr Institute, University of Copenhagen, Copenhagen, Denmark*

[4] *Department of Environmental Sciences, Informatics and Statistics, University Ca' Foscari of Venice, Venice, Italy*

[5] *Department of Mechanical and Process Engineering, ETH Zurich, 8092 Zurich, Switzerland*

Abstract

Stable water isotopes ($\delta^{18}O$) obtained from snow and ice samples of polar regions are used to reconstruct past climate variability, but heat and mass transport processes can affect the isotopic composition. Here we present an experimental study on the effect of airflow on the snow isotopic composition through a snow pack in controlled laboratory conditions. The influence of isothermal and controlled temperature gradient conditions on the $\delta^{18}O$ content in the snow and interstitial water vapor is elucidated. The observed disequilibrium between snow and vapor isotopes led to the exchange of isotopes between snow and vapor under non-equilibrium processes, significantly changing the $\delta^{18}O$ content of the snow. The type of metamorphism of the snow had a significant influence on this process. These findings are pertinent to the interpretation of the records of stable isotopes of water from ice cores. These laboratory measurements

[*] Corresponding author. Email: schneebeli@slf.ch

suggest that a highly resolved climate history is relevant for the interpretation of the snow isotopic composition in the field.

Keywords: snow, isotope, isothermal, metamorphism, advection, tomography, post-depositional process

1. Introduction

Water stable isotopes in polar snow and ice have been used for several decades as proxies for global and local temperatures (e.g. Dansgaard, 1964; Lorius et al., 1979; Grootes et al., 1994; Petit et al., 1999; Johnsen et al., 2001; EPICA Members, 2004). However, the processes that influence the isotopic composition of precipitation in high-latitude are complex, making direct inference of paleo temperatures from the isotopic record difficult (Cuffey et al., 1994; Jouzel et al., 1997, 2003; Hendricks et al., 2000). Several factors affect the vapor and snow isotopic composition, which give rise to ice core isotopic composition, starting from the process of evaporation in the source region, transportation of the air mass to the top of the ice sheet, and post-depositional processes (Craig and Gordon, 1964; Merlivat and Jouzel, 1979; Johnsen et al. 2001; Ciais and Jouzel, 1994; Jouzel and Merlivat, 1984; Jouzel et al., 2003; Helsen et al., 2005, 2006, 2007; Cuffey and Steig, 1998; Krinner and Werner, 2003). Mechanical processes such as mixing, seasonal scouring, or spatial redistribution of snow can alter seasonal and annual records (Fisher et al., 1983; Hoshina et al., 2014). Post-depositional processes associated with wind scouring and snow redistribution are known to introduce a "post-depositional noise" in the surface snow. Comparisons of isotopic records obtained from closely located shallow ice cores have allowed for estimation of a signal-to-noise ratio

and a common climate signal (Fisher and Koerner, 1988, 1994; White et al., 1997; Steen-Larsen et al., 2011; Sjolte et al., 2011; Masson-Delmotte et al., 2015). After deposition, interstitial diffusion in the firn and ice affects the water-isotopic signal but back-diffusion or deconvolution techniques have been used to establish the original isotope signal (Johnsen, 1977; Johnsen et al., 2000).

Snow is a bi-continuous material consisting of fully connected ice crystals and pore space (air) (Löwe et al., 2011). Because of the proximity to the melting point, the high vapor pressure causes a continuous recrystallization of the snow microstructure known as snow metamorphism, even under moderate temperature gradients (Pinzer et al., 2012). The whole ice matrix is continuously recrystallizing by sublimation and deposition, with vapor diffusion as the dominant transport process. Pinzer et al. (2012) showed that a typical half-life of the ice matrix is a few days. The intensity of the recrystallization is dictated by the temperature gradient and this can occur under mid-latitude or polar conditions. Temperature, and geometrical factors (porosity and specific surface area) also play a significant role (Pinzer and Schneebeli, 2009; Pinzer et al., 2012).

The interpretation of ice core data and the comparison with atmospheric model results implicitly rely on the assumption that the snowfall precipitation signal is preserved in the snow-ice matrix (Werner et al., 2011). Classically, ice-core stable-isotope records are interpreted as reflecting precipitation-weighted signals, and compared to observations and atmospheric model results for precipitation, ignoring snow-vapor exchanges between surface snow and atmospheric water vapor (e.g. Persson et al., 2011). However, recent studies carried out on top of the Greenland and Antarctic ice sheets combining continuous atmospheric water vapor isotope observations with daily snow surface sampling document a clear day-to-day variation of isotopic

composition of surface snow between precipitation events as well as diurnal change in the snow isotopes (Steen-Larsen et al., 2014a; Ritter et al., 2016; Casado et al., 2016). This effect was interpreted as being caused by the uptake of the synoptic-driven atmospheric water-vapor isotope signal by individual snow crystals undergoing snow metamorphism (Steen-Larsen et al., 2014a) and the diurnal variation in moisture flux (Ritter et al., 2016). However, the impact of this process on the isotope-temperature reconstruction is not yet sufficiently understood, but crucial to constrain. This process, compared to interstitial diffusion (Johnsen, 1977; Johnsen et al., 2000), will alter the isotope mean value. The field observations challenge the previous assumption that sublimation occurred molecular layer-by-layer with no resulting isotopic fractionation (Dansgaard, 1964; Friedman et al., 1991; Town et al., 2008; Neumann and Waddington, 2004). It is assumed that the solid undergoing sublimation would not be unduly enriched in the heavier isotope species due to the preferential loss of lighter isotopic species to the vapor (Dansgaard, 1964; Friedman et al., 1991). Because self-diffusion in the ice is about three orders of magnitude slower than molecular diffusion in the vapor, the amount of isotopic separation in snow is assumed to be negligible.

Snow has a high permeability (Calonne et al., 2012; Zermatten et al., 2014), which facilitates diffusion of gases and, under appropriate conditions, airflow (Gjessing, 1977; Colbeck, 1989; Sturm and Johnson, 1991; Waddington et al., 1996). In a typical Antarctic and Greenland snow profile, strong interactions between the atmosphere and snow occurs, especially in the first 2 m (Neumann and Waddington, 2004; Town et al., 2008), called the convective zone. In the convective zone, air can move relatively freely and therefore exchange between snow and the atmospheric air occurs. Air flowing into the snow reaches saturation vapor pressure nearly instantly through sublimation (Neumann et al., 2008; Ebner et al., 2015a). Models of the influence of the so-called

98 'wind pumping'-effect (Fisher et al., 1983; Neumann and Waddington, 2004), in which
99 the interstitial water vapor is replaced by atmospheric air pushed through the upper
100 meters of the snow pack by small-scale high and low pressure areas caused by irregular
101 grooves or ridges formed on the snow surface (dunes and sastrugi), have assumed that
102 the snow grains would equilibrate with the interstitial water vapor on timescales
103 governed by ice self-diffusion. However, no experimental data are available to support
104 this assumption. With this in mind the experimental study presented here is specifically
105 developed to investigate the effect of ventilation inside the snow pack on the isotopic
106 composition. Only conditions deeper than 1 cm inside a snowpack are considered.
107 Previous work showed that (1) under isothermal conditions, the Kelvin effect leads to a
108 saturation of the pore space in the snow but does not affect the structural change (Ebner
109 et al., 2015a); (2) applying a negative temperature gradient along the flow direction
110 leads to a change in the microstructure due to deposition of water molecules on the ice
111 matrix (Ebner et al., 2015b); and (3) a positive temperature gradient along the flow had
112 a negligible total mass change of the ice but a strong reposition effect of water
113 molecules on the ice grains (Ebner et al., 2016). Here, we continuously measured the
114 isotopic composition of an airflow containing water vapor through a snow sample under
115 both isothermal and temperature gradient conditions. Micro computed-tomography
116 (μCT) was applied to obtain the 3D microstructure and morphological properties of
117 snow.

118 **2. Experimental setup**

119 Isothermal and temperature gradient experiments with fully saturated airflow and
120 defined isotopic composition were performed in a cold laboratory at around $T_{lab} \approx$ -15
121 °C with small fluctuations of ± 0.8 °C (Ebner et al., 2014). Snow produced from de-
122 ionized tap water in a cold laboratory (water temperature: 30 ºC; air temperature: -20

ºC) was used for the snow sample preparation (Schleef et al., 2014). The snow was sieved with a mesh size of 1.4 mm into a box, and isothermally sintered for 27 days at -5 ºC to increase the strength, in order to prevent destruction of the snow sample due to the airflow, and to evaluate the effect of metamorphism of snow. The morphological properties of the snow are listed in Table 1. The sample holder (diameter 53 mm, height 30 mm, 0.066 liter) was filled by a cylinder cut out from the sintered snow. To prevent air flow between snow sample and the sample holder walls, the undisturbed snow disk was filled in at a higher temperature (about -5 °C) and sintering was allowed for about 1 h before cooling down and start of the experiment. The setup of Ebner et al. (2014) was modified by additionally inserting a water vapor isotope analyzer (Model: L1102-I Picarro, Inc., Santa Clara, CA, USA) to measure the isotopic ratio $\delta^{18}O$ of the water vapor contained in the airflow at the inlet and outlet of the sample holder. The experimental setup consisted of three main components (humidifier, sample holder, and the Picarro analyzer) connected with insulated copper tubing and Swagelok fitting (Fig. 1). The tubes to the Picarro analyzer were heated to prevent deposition of water vapor and thereby fractionation. The temperature was monitored with thermistors inside the humidifier and at the inlet and outlet of the snow sample. A dry air pressure tank controlled by a mass flow controller (EL-Flow, Bronkhorst) generated the airflow. A humidifier, consisting of a tube (diameter 60 mm, height 150 mm, 0.424 liter volume) filled with crushed ice particles (snow from Antarctica with low $\delta^{18}O$ composition), was used to saturate the dry air entering the humidifier with water vapor at an almost constant isotopic composition. The air temperature in the humidifier and at the inlet of the snow sample was maintained at the same value (accuracy ± 0.2 K) to limit the influence of variability in absolute vapor pressure and isotopic composition. We measured the $\delta^{18}O$ of the water vapor produced by the humidifier before and after each

148 experimental run ($\delta^{18}O_{hum}$). The outlet flow ($\delta^{18}O_a$) of the sample holder was
149 continuously measured during the experiment to analyze the temporal evolution of the
150 isotopic signal. All data from the Picarro analyzer were corrected to the humidity
151 reference level using the established instrument humidity-isotope response (Steen-
152 Larsen et al. 2013; 2014b). In addition, VSMOW-SLAP correction and drift correction
153 were performed. We followed the calibration protocol and used the calibration system
154 described in detail by Steen-Larsen et al. (2013; 2014b).

155 The sample holder described by Ebner et al. (2014) was used to analyze the snow by
156 μCT. Tomography measurements were performed with a modified μ-CT80 (Scanco
157 Medical). The equipment incorporated a microfocus X-ray source, operated at 70 kV
158 acceleration voltage with a nominal resolution of 18 μm. The samples were scanned
159 with 1000 projections per 180º in high-resolution setting, with typical adjustable
160 integration time of 200 ms per projection. The field of view of the scan area was 36.9
161 mm of the total 53 mm diameter, and subsamples with a dimension of 7.2 × 7.2 × 7.2
162 mm^3 were extracted for further processing. The reconstructed μCT images were filtered
163 using a 3 × 3 × 3 median filter followed by a Gaussian filter (σ = 1.4, support = 3). The
164 Otsu method (Otsu, 1979) was used to automatically perform clustering-based image
165 thresholding to segment the grey-level images into ice and void phase. Morphological
166 properties in the two-phase system were determined based on the exact geometry
167 obtained by the μCT. Tetrahedrons corresponding to the enclosed volume of the
168 triangulated ice matrix surface were applied on the segmented data to determine
169 porosity (ε) and specific surface area (SSA). The mean pore size distribution was
170 estimated using the opening-size-distribution operation. This operation can be imagined
171 as virtual sieving with different mesh size (Haussener et al., 2012).

Three experiments with saturated advective airflow through the snow sample were performed to record the following parameters and analyze their effects: (1) isothermal conditions to analyze the influence of curvature effects (Kaempfer al et., 2007); (2) positive temperature gradient applied to the snow sample where cold air entering the sample is heated while flowing through the sample in order to analyze the influence of sublimation; (3) negative temperature gradient applied to the snow sample where warm air entering the sample is cooled while flowing across the sample, to analyze the influence of net deposition. During the temperature gradient experiments, a temperature difference of 1.4 ºC and 1.8 ºC was imposed resulting in a gradient of +47 K m^{-1} and -60 K m^{-1}, respectively. The runs were performed at atmospheric pressure and with a volume flow rate of 3.0 liter min^{-1} corresponding to an average flow speed in the pores of $u_D \approx 30$ mm s^{-1}. We performed the experiments with airflow velocities in the snow sample at $u_D \approx 30$ mm s^{-1}, which is a factor of three higher than calculated by Neumann (2003) for a natural snow pack. But looking at the Reynolds number, describing the flow regime inside the pores, our experiments (Re ≈ 0.7) were in the feasible flow regime (laminar flow) of a natural snow pack (Re ≈ 0.65). In experiment (2) the outlet temperature and in experiment (3) the inlet and also the humidifier temperature were actively controlled using thermo-electric elements. Variations in temperature of up to ± 0.8 ºC were due to temperature fluctuations inside the cold laboratory, leading to slightly variable temperature gradients and mean temperature in experiment (2) and (3). Table 1 presents a summary of the experimental conditions and the morphological properties of the snow samples. All snow samples were taken from the same snow block with an average density of ≈ 210 kg m^{-3}. The density given in Table 1 was the density of the snow sample in each experiment measured by μCT. At the end of each experiment, the snow sample was cut into five layers of 6 mm height and the isotopic composition of

each layer was analyzed to examine the spatial $\delta^{18}O$ gradient in the isotopic composition of the snow sample.

A slight increase with a maximum of 0.7 ‰ of $\delta^{18}O$ in the water vapor produced by the humidifier was observed in experiment (1), with lower increases during experiments (2) and (3) (Table 2). This change of ~0.7‰ is not significant compared to the difference between the isotopic composition of the water vapor and the snow sample in the sample holder of ~53‰ and the temporal change of the water vapor isotopes on the back side of the snow sample.

In the first approximately 30 min, the isotopic composition of the measured outflow air $\delta^{18}O_a$ increased from a low $\delta^{18}O$ to a starting value of around -29‰ in each experiment. This was due to memory effect and one possible effect might be condensed water left in the tubes from a prior experiment which had no further impact on the experiments (Penna et al., 2012).

3. Results

3.1 Isothermal condition

The experiment (1) was performed for 24 h at a mean temperature of T_{mean} = -15.5 ºC. $\delta^{18}O_a$ decreased exponentially in the outlet flow observed throughout the experimental run as shown in Fig. 2. Initially, the $\delta^{18}O_a$ content in the flow was -27.7 ‰ and exponentially decreased to -47.6 ‰ after 24 h. The small fluctuations in the $\delta^{18}O_a$ signal at $t \approx 7$ h, 17 h and 23 h were due to small temperature changes in the cold laboratory.

We observed a strong interaction between the airflow and the snow as manifest by the isotopic composition of the snow. The $\delta^{18}O_s$ signal in the snow decreased by 4.75 – 7.78 ‰ and an isotopic gradient in the snow was observed after the experimental run,

shown in Fig. 3. Initially, the snow had a homogeneous isotopic composition of $\delta^{18}O_s$ = -10.97 ‰ but post-experiment sampling showed a decrease in the snow $\delta^{18}O$ at the inlet side to -17.75 ‰ and at the outlet side to -15.72 ‰. The spatial $\delta^{18}O_s$ gradient of the snow had an approximate slope of 0.68 ‰ mm^{-1} at the end of the experimental run. Table 2 shows the $\delta^{18}O$ value in snow at the beginning (t = 0) and end (t = 24 h) of the experiment.

3.2 Air warming by a positive temperature gradient along the airflow

The experiment (2) was performed over a period of 24 h with an average temperature gradient of approximatively +47 K m^{-1} (warmer temperatures at the outlet of the snow) and an average mean temperature of -14.7 ºC. As in the isothermal experiment (1), we observed a relaxing exponential decrease of $\delta^{18}O_a$ in the outlet flow throughout the measurement period as shown in Fig. 2, but the decrease was slower compared to the isothermal run. Initially, the $\delta^{18}O_a$ content in the flow coming through the snow disk was -29.8 ‰ and exponentially decreased to -41.9 ‰ after 24 h. The small fluctuations in the $\delta^{18}O_a$ signal at $t \approx 2.7$ h, and 12.7 h were due to small temperature changes in the cold laboratory.

The $\delta^{18}O_s$ signal in the snow decreased 4.66 – 7.66 ‰ and a gradient in the isotopic composition of the snow was observed after the experimental run, shown in Fig. 3. Initially, the snow had a homogeneous isotopic composition of $\delta^{18}O_s$ = -11.94 ‰, but post-experiment sampling showed a decrease at the inlet side to -19.6 ‰ and at the outlet side to -16.6 ‰. The spatial $\delta^{18}O_s$ gradient of the snow had an approximate slope of 1.0 ‰ mm^{-1} at the end of the experimental run. Table 2 shows the $\delta^{18}O_s$ value in snow at the beginning (t = 0) and end (t = 24 h) of the experiment.

3.3 Air cooling by a negative temperature gradient along the air flow

The experiment (3) was performed for 84 h instead of 24 h to better estimate the trend in $\delta^{18}O_a$ in the outlet flow. An average temperature gradient of approximately -60 K m^{-1} (colder temperatures at the outlet of the snow) and an average mean temperature of -13.2 ºC were observed during the experiment. As in the previous experiments, a relaxing exponential decrease of $\delta^{18}O_a$ in the outlet flow was observed throughout the experimental run as shown in Fig. 2, but the decrease was slower compared to the isothermal run and temperature gradient opposed to the airflow. Initially, the $\delta^{18}O_a$ content in the flow was -29.8 ‰ and exponentially decreased to -37.7 ‰ after 84 h. The small fluctuations in the $\delta^{18}O_a$ signal at $t \approx 7.3$ h, 21.3 h, 31.3 h, 45.3 h, 55.3 h, 69.3 h, and 79.3 h were due to small temperature changes in the cold laboratory.

The $\delta^{18}O_s$ signal in the snow decreased 4.46 – 15.09 ‰ and a gradient in the isotopic composition of the snow was observed after the experimental run, shown in Fig. 3. Initially, the snow had an isotopic composition of $\delta^{18}O_s$ = -10.44 ‰ but post-experiment sampling showed a decrease at the inlet side to -25.53 ‰ and at the outlet side to -15.00 ‰. The spatial $\delta^{18}O_s$ gradient of the snow had an approximate slope of 3.5 ‰ mm^{-1} at the end of the experimental run. Table 2 shows the $\delta^{18}O_s$ value in snow at the beginning (t = 0) and end (t = 84 h) of the experiment.

4. Discussion

All experiments showed a strong exchange in $\delta^{18}O$ between the snow and water-vapor saturated air resulting in a significant change of the value of the stable isotopes in the snow. The advective conditions in the experiments were comparable with surface snow layers in Antarctica and Greenland, but at higher temperature, especially compared to interior Antarctica.

The results also showed strong interactions in $\delta^{18}O$ between snow and air depending on the different temperature gradient conditions. The experiments indicate that

temperature variation and airflow above and through the snow structures (Sturm and Johnson, 1991; Colbeck, 1989; Albert and Hardy, 1995) seem to be dominant processes affecting water stable isotopes of surface snow. The results also support the statement that an interplay between theoretically expected layer-by-layer sublimation and deposition at the ice-matrix surface and the isotopic content evolution of snow cover due to mass exchange between the snow cover and the atmosphere occurs (Sokratov and Golubev, 2009). The specific surface area of snow exposed to mass exchange (Horita et al., 2008) and by the depth of the snow layer exposed to the mass exchange with the atmosphere (He and Smith, 1999) plays an important role. Our results support the interpretation that changes in surface snow isotopic composition are expected to be significant if large day-to-day surface changes in water vapor occur in between precipitation events, wind pumping is efficient and snow metamorphism is enhanced by temperature gradients in the upper first centimeters of the snow (Steen-Larsen et al., 2014a).

We expect that our findings will lead to improvement of the interpretation of the water stable isotope records from ice cores. Classically, ice core stable isotope records are interpreted as paleo-temperature reflecting precipitation-weighted signals. When comparing observations and atmospheric model results for precipitation with ice core records, such vapor-snow exchanges are normally ignored (e.g. Persson et al., 2011; Fujita and Abe, 2006). However, vapor-snow exchange enhanced by recrystallization rate seems to be an important factor for the high variation in the snow surface $\delta^{18}O$ signal as supported by our experiments. It was hypothesized that the changes in the snow-surface $\delta^{18}O$ reported by Steen-Larsen et al. (2014a) are caused by changes in large-scale wind and moisture advection of the atmospheric water vapor signal and

294 snow metamorphism. The strong interaction between atmosphere and near-surface snow
295 can modify the ice core water stable isotope records.

296 The rate-limiting step for isotopic exchange in the snow is isotopic equilibration
297 between the pore-space vapor and surrounding ice grains. The relaxing exponential
298 decrease of $\delta^{18}O$ in the outflow of our experiments predicted that full isotopic
299 equilibrium between snow and atmospheric vapor will not be reached at any depth
300 (Waddington et al., 2002; Neumann and Waddington, 2004) but changes towards
301 equilibrium with the atmospheric state occurs (Steen-Larsen et al., 2013, 2014a).

302 As snow accumulates, the upper 2 m are advected through the ventilated zone
303 (Neumann and Waddington, 2004; Town et al., 2008). In areas with high accumulation
304 rate (e.g. South Greenland), snow is advected for a short time through the ventilated
305 zone. The snow exposed a relatively short time to vapor snow exchange would result in
306 higher spatial variability compared to long-time exposure. However, the effects of snow
307 ventilation on isotopic composition may become more important as the accumulation
308 rate of the snow decreases (< 50 mm a^{-1}), such that snow remains in the near-surface
309 ventilated zone for many years (Waddington et al., 2002; Hoshina et al., 2014; Hoshina
310 et al., 2016). As the snow remains longer in the near-surface ventilated zone, a larger
311 $\delta^{18}O$ exchange between snow and atmospheric vapor will occur. Consequently, the
312 isotopic content of layers at sites with high and low accumulation rates can evolve
313 differently, even if the initial snow composition had been equal, and the sites had been
314 subjected to the same histories of air-mass vapor.

315 Despite a relatively small change in the difference between the isotopic composition
316 of the incoming vapor and the snow, large differences in the isotopic composition of the
317 water vapor at the outlet flow exist for the three different experimental setups. Based on
318 the difference in the outlet water vapor isotopic composition, we hypothesized that

319 different processes are at play for the different experiments. It is obvious that there is a
320 fast isotopic exchange with the surface of the ice crystals, and a much slower timescale
321 on which the interior of the ice crystals is altered. Due to the low diffusivity of $H_2{}^{16}O$
322 and $H_2{}^{18}O$ in ice ($D_{H_2{}^{18}O} \approx D_{H_2{}^{16}O} = \sim 10^{-15}$ m^2 s^{-1} (Ramseier, 1967; Johnsen et al., 2000),
323 we assumed that the interior of the ice crystals is not altered on the timescale of the
324 experiment. This explained why the net isotopic change of the bulk sample is relatively
325 small compared to the changes in the outlet water vapor isotopes. The effective 'ice-
326 diffusion depth' of the isotopic exchange during the experiments is given as $L_D = \sqrt{D \cdot t}$,
327 where D is the diffusion coefficient of $H_2{}^{16}O$ and $H_2{}^{18}O$ in ice, respectively, and t the
328 experimental time. The calculated 'ice-diffusion depth' L_D, is ~ 9.3 μm for experiments
329 (1) and (2), and ~17.4 μm for experiment (3), respectively, indicating an expected a
330 minimal change of the interior of the ice crystal. However, snow has a large specific
331 surface area and therefore a high exchange area. This has an effect on the $\delta^{18}O$ snow
332 concentration. The fraction of the total volume V_{tot} of ice that is close enough to the ice
333 surface to be affected by diffusion in time t is then $\rho_{ice} \cdot SSA \cdot L_D$, where SSA is the
334 specific surface area (area per unit mass), and L_D is the diffusion depth, defined above,
335 for time t. For $t \approx 24$ hours, a large fraction (24 to 43 %) of the total volume V_{tot} of the
336 ice matrix can be accessed through diffusion. It is quite hard to see the total $\delta^{18}O$ snow
337 difference between experiments (1) and (2) after the experiment compared to the $\delta^{18}O$
338 of the vapor in the air at the outlet. There is a small, but notable, difference in the total
339 $\delta^{18}O$ of the snow between experiment (1) and (2). Due to the higher recrystallization
340 rate of experiment (2) the spatial $\delta^{18}O_s$ gradient of the snow (1.0 ‰ mm^{-1}) is higher than
341 for experiment (1) (0.68 ‰ mm^{-1}). Increasing the experimental time, the $\delta^{18}O$ change in
342 the snow increases (experiment (3)). In general, the calculated 'ice-diffusion depth' is
343 realistic under isothermal conditions where diffusion processes are the main factors

(Kaempfer and Schneebeli, 2007; Ebner et al., 2015). Applying a temperature gradient, the impact of diffusion is suppressed due to the high recrystallization rate by sublimation and deposition. Due to the low half-life of the ice matrix of a few days, the growth rates are typically on the order of 100 μm per day (Pinzer et al., 2012). Therefore, this redistribution of ice caused by temperature gradient counteracts the diffusion into the solid ice.

By comparing similarities and differences between the outcomes of the three experimental setups we will now discuss the physical processes influencing the interaction and exchange processes within the snowpack between the snow and the advected vapor. We first notice that the final snow isotopic profile of experiment (1) (isothermal) and (2) (positive temperature gradient along the direction of the flow) are comparable to each other. Despite this similarity, the evolution in the outlet water vapor of experiment (1) showed a significantly stronger depletion compared to experiment (2). For experiment (3) (negative temperature gradient along the direction of the flow) we observed the smallest change in outlet water vapor isotopes but the largest snow-pack isotope gradient after the experiment. However, this change was caused by 84 hours flow instead of 24 hours.

Curvature effects, temperature gradients and therefore the recrystallization rate influence the mass transfer of $H_2{}^{16}O$/ $H_2{}^{18}O$ molecules. The higher the recrystallization rate of the snow the slower the adaption of the outlet air concentration to the inlet air concentration (see in experiment (2) and (3)). Under isothermal conditions (experiment (1)) the only effect influencing the recrystallization rate is the curvature effect (Kaempfer and Schneebeli, 2007). However, based on the experimental observations (Kaempfer and Schneebeli, 2007) this effect decreases with decreasing temperature and increasing experimental time. Applying an additional temperature gradient on a snow

sample causes complex interplays between local sublimation and deposition on surfaces and the interaction of water molecules in the air with the ice matrix due to changing saturation conditions of the airflow. Therefore, the recrystallization rate increases and causes the change in the $\delta^{18}O$ of the air. For experiment (2) there is a complex interplay between sublimation and deposition of water molecules into the interstitial flow (Ebner et al., 2015c) while for experiment (3) there is deposition of molecules carried by the interstitial flow onto the snow crystals (Ebner et al., 2015b). Furthermore, in the beginning of each experiment there is a tendency to sublimate from edges of the individual snow crystals due to the higher curvature. As the edges were sublimated and deposition occurred in the concavities, the individual snow crystals became more rounded, slowing down the transfer of water molecules into the interstitial airflow. We noticed for all three experiments that within the uncertainty of the isotopic composition of the snow, the initial isotopic composition of the vapor was the same and in isotopic equilibrium with the snow. The difference between experiment (1) and (2) lies in the fact that due to the temperature gradient in experiment (2) there is an increased transfer of water vapor with the isotopic composition of the snow into the airflow. Hence the depleted air from the humidifier advected through the snow disk is mixed with a relatively larger vapor flux from the snow crystals. Additionally, we also expected less deposition into the concavities in experiment (2) compared to experiment (1). However, it is interesting to note that the final isotopic profile of the snow disk is similar in experiment (1) and experiment (2). We interpreted this as being a result of two processes acting in opposite direction: although relatively isotope-depleted vapor from the humidifier was deposited on the ice matrix there was also a higher amount of sublimation of relatively isotope-enriched vapor from the snow disk in experiment (2). Experiment (3) separates itself from the other two experiments in the way that as the

water vapor from the humidifier is advected through the snow disk there is a continuous deposition of very depleted air due the negative temperature gradient. As for the case of experiment (1) and (2) there was also in experiment (3) a constant sublimation of the convexities into the vapor stream. We notice that despite the fact that experiment (3) ran for 84 hours the snow at the outlet side of the snow-disk did not become more isotopically depleted compared to experiment (1) and (2). However, the snow on the inlet side became significantly more isotopically depleted. This observation, together with the fact that the vapor of the outlet of the snow-disk is less depleted compared to experiment (1) and (2), leads us to hypothesize that there is a relatively larger deposition of isotopically depleted vapor from the humidifier as the vapor is advected through the snow disk. This means that a relatively larger component of the isotopic composition of the vapor is originating by sublimation from the convexities of the snow disk and less from the isotopically depleted vapor from the humidifier.

Our results and conclusions indicate that there is a need for additional validation. Specifically, it would be crucial to know the mass balance of the snow disk more precisely, which could be done by reconstructing the entire snow disk following the change in density and morphological properties over the entire height. Ideally, the entire sample would be tomographically measured with a resolution of 4 x 4 x 4 mm^3, each cube corresponding to the representative volume. Insights would also be achieved with experiments using snow of the same isotopic composition, but different SSA, as more precise calculation of the different observed exchange rates would be allowed. Additionally, different and colder background temperatures should be tested to better understand inland Antarctic environment and the effect of the quasi-liquid layer, which is necessary for the development of a numerical model. Isotopically different combinations of vapor and snow should be performed. In the present manuscript, vapor

with low $\delta^{18}O$ isotopic composition was transported through snow with relative high $\delta^{18}O$ isotopic composition. It would be interesting to reverse the combination and perform experiments with different combinations to provide more insights on mass and isotope exchanges between vapor and snow. Experiments with longer running time help to understand the change in the ice matrix better under low accumulation conditions.

4. Summary and conclusion

Laboratory experimental runs were performed where a transient $\delta^{18}O$ interaction between snow and air was observed. The airflow altered the isotopic composition of the snowpack and supports an improved climatic interpretation of ice core stable water isotope records. The water vapor saturated airflow with an isotopic difference of up to 55‰ changed within 24 h and 84 h the original $\delta^{18}O$ isotope signal in the snow by up to 7.64 ‰ and 15.06 ‰. The disequilibrium between snow and air isotopes led to the observed exchange of isotopes, the rate depending on the temperature gradient conditions. Concluding, increasing the recrystallization rate in the ice matrix causes the temporal change of the $\delta^{18}O$ concentration at the outflow to decrease (experiment (2) and (3)). Decreasing the recrystallization rate causes the temporal curve of the outlet concentration to become steeper reaching the $\delta^{18}O$ inlet concentration of the air faster (experiment (1)).

Additionally, the complex interplay of simultaneous diffusion, sublimation and deposition due to the geometrical complexity of snow has a strong effect on the $\delta^{18}O$ signal in the snow and cannot be neglected. A temporal signal can be superimposed on the precipitation signal, (a) if the snow remains near the surface for a long time, i.e. in a low-accumulation area, and (b) is exposed to a history of air masses carrying vapor with a significantly different isotopic signature than the precipitated snow.

These are novel measurements and will therefore be important as the basis for further research and experiments. Our results represent direct experimental observation of the interaction between the water isotopic composition of the snow, the water vapor in the air and recrystallization due to temperature gradients. Our results demonstrate that recrystallization and bulk mass exchange must be incorporated into future models of snow and firn evolution. Further studies are required on the influence of temperature and airflow as well as snow microstructure on the mass transfer phenomena for validating the implementation of stable water isotopes in snow models.

Acknowledgements

The Swiss National Science Foundation granted financial support under project Nr. 200020-146540. H.C. Steen-Larsen was supported by the AXA Research Fund. The authors thank K. Fujita, E. D. Waddington and an anonymous reviewer for the suggestions and critical review. M. Jaggi, S. Grimm, A. Schlumpf, and S. Berben gave technical support. The data for this paper are available by contacting the corresponding author.

References

Albert M. R. and Hardy J. P.: Ventilation experiments in a seasonal snow cover, in Biogeochemistry of Seasonally Snow-Covered Catchments, IAHS Publ. 228, edited by K. A. Tonnessen, M. W. Williams, and M. Tranter, 41–49, IAHS Press, Wallingford, UK, 1995.

Calonne N., Geindreau C., Flin F., Morin S., Lesaffre B., Rolland du Roscoat S., and Charrier P.: 3-D image-based numerical computations of snow permeability: links

468 to specific surface area, density, and microstructural anisotropy, The Cryosphere, 6,
469 939-951, 2012.
470 Casado M., Landais A., Masson-Delmotte V., Genthon C., Kerstel E., Kassi S., Arnaud
471 L., Picard G., Prie F., Cattani O., Steen-Larsen H. C., Vignon E., and Cermak P.:
472 Continuous measurements of isotopic composition of water vapour on the East
473 Antarctic Plateau, Atmos. Chem. Phys. Discuss., doi:10.5194/acp-2016-8, in
474 review, 2016.
475 Ciais P., and Jouzel J.: Deuterium and oxygen 18 in precipitation: Isotopic model,
476 including mixed-cloud processes, Journal of Geophysical Research, 99, 16793–
477 16803, doi:10.1029/94JD00412, 1994.
478 Colbeck S. C.: Air movement in snow due to windpumping, Journal of Glaciology, 35,
479 209–213, 1989.
480 Craig H. and Gordon L. I.: Deuterium and oxygen 18 variations in the ocean and marine
481 atmosphere, In proc. Stable Isotopes in Oceanographic Studies and
482 Paleotemperatures, (ed. E. Toniorgi), Spoleto, Italy, 9–130, 1964.
483 Cuffey K. M. and Steig E. J.: Isotopic diffusion in polar firn: Implications for
484 interpretation of seasonal climate parameters in ice-core records, with emphasis on
485 central Greenland, Journal of Glaciology, 44, 273–284, 1998.
486 Cuffey K. M., Alley R. B., Grootes P. M., Bolzan J. M., and Anandakrishnan S.:
487 Calibration of the Delta-O-18 isotopic paleothermometer for central Greenland,
488 using borehole temperatures, Journal of Glaciology, 40, 341–349, 1994.
489 Dansgaard W.: Stable isotopes in precipitation, Tellus, 16, 436–468, 1964.
490 Ebner P. P., Grimm S., Schneebeli M., and Steinfeld A.: An instrumented sample holder
491 for time-lapse micro-tomography measurements of snow under advective

conditions, Geoscientific Instrumentation Methods and Data Systems, 3, 179–185, doi:10.5194/gi-3-179-2014, 2014.

Ebner P. P, Schneebeli M., and Steinfeld A. Tomography-based observation of isothermal snow metamorphism under advective conditions, The Cryosphere, 9, 1363–1371, 2015a.

Ebner P. P, Andreoli C., Schneebeli M., and Steinfeld A.: Tomography-based characterization of ice-air interface dynamics of temperature gradient snow metamorphism under advective conditions, Journal of Geophysical Research, Journal of Geophysical Research Earth Surface, 120, doi:10.1002/2015JF003648, 2015b.

Ebner P. P., Schneebeli M., and Steinfeld A.: Metamorphism during temperature gradient with undersaturated advective airflow in a snow sample, The Cryosphere, 10, 791-797, 2016.

EPICA Members: Eight glacial cycles from an Antarctic ice core, Nature, 429, 623–628, doi:10.1038/nature02599, 2004.

Gjessing Y. T.: The filtering effect of snow, in: Isotopes and Impurities in Snow and Ice Symposium, edited by: Oeschger, H., Ambach, W., Junge, C. E., Lorius, C., and Serebryanny, L., IASHAISH Publication, Dorking, 118, 199–203, 1977.

Grootes P. M., Steig E., and Stuiver M.: Taylor Ice Dome study 1993-1994: An ice core to bedrock, Antarctic Journal U.S., 29, 79–81, 1994.

Fisher D. A., Koerner R. M., Paterson W. S. B., Dansgaard W., Gundestrup N., and Reeh N.: Effect of wind scouring on climatic records from ice-core oxygen-isotope profiles, Nature, 301, 205–209, doi:10.1038/301205a0, 1983.

515 Fisher D. A. and Koerner R.: The effect of wind on d(18O) and accumulation given an
516 inferred record of seasonal d amplitude from the Agassiz ice cap, Ellesmere island,
517 Canada, Annals of Glaciology, 10, 34–37, 1988.
518 Fisher D. A. and Koerner R.: Signal and noise in four ice-core records from the Agassiz
519 ice cap, Ellesmere Island, Canada: Details of the last millennium for stable
520 isotopes, melt and solid conductivity, The Holocene, 4, 113–120,
521 doi:10.1177/095968369400400201, 1994.
522 Friedman I., Benson C., and Gleason J.: Isotopic changes during snow metamorphism,
523 in Stable Isotope Geochemistry: A Tribute to Samuel Epstein, edited by J. R.
524 O'Neill and I. R. Kaplan, pp. 211–221, Geochemical Society, Washington, D. C.,
525 1991.
526 Haussener S., Gergely M., Schneebeli M., and Steinfeld A.: Determination of the
527 macroscopic optical properties of snow based on exact morphology and direct pore-
528 level heat transfer modeling, Journal of Geophysical Research, 117, 1–20,
529 doi:10.1029/2012JF002332, 2012.
530 He H. and Smith R. B.: An advective-diffusive isotopic evaporation-condensation
531 model, Journal of Geophysical Research, 104, 18619-18630,
532 doi:10.1029/1999JD900335, 1999.
533 Helsen M. M., van de Wal R. S. W., van den Broeke M. R., van As D., Meijer H. A. J.,
534 and Reijmer C. H.: Oxygen isotope variability in snow from western Dronning
535 Maud Land, Antarctica and its relation to temperature, Tellus, 57, 423–435, 2005.
536 Helsen M. M., van de Wal R. S. W., van den Broeke M. R., Masson-Delmotte V.,
537 Meijer H. A. J., Scheele M. P., and Werner M., Modeling the isotopic composition
538 of Antartic snow using backward trajectories: Simulation of snow pit records,
539 Journal of Geophysical Research, 111, doi:10.1029/2005JD006524, 2006.

Helsen M. M., van de Wal R. S. W., and van den Broeke M. R.: The isotopic composition of present-day Antartic snow in a Lagrangian simulation, Journal of Climate, 20, 739–756, 2007.

Hendricks M. B., DePaolo D. J., and Cohen R. C.: Space and time variation of $\delta^{18}O$ and δD in precipitation: Can paleotemperature be estimated from ice cores?, Global Biogeochemical Cycles, 14, 851–861, doi:10.1029/1999GB001198, 2000.

Horita J., Rozanski K., and Cohen S.: Isotope effects in the evaporation of water: a status report of the Craig-Gordon model, Isotopes in Environmental Health Studies, 44, 23-49, doi:10.1080/10256010801887174, 2008.

Hoshina Y., Fujita K., Nakazawa F., Iizuka Y., Miyake T., Hirabayashi M., Kuramoto T., Fujita S., and Motoyama H.: Effect of accumulation rate on water stable isotopes of near-surface snow in inland Antarctica. Journal of Geophysical Research - Atmospheres, 119(1), 274-283. doi:10.1002/2013JD020771, 2014.

Hoshina Y., Fujita K., Iizuka Y., Motoyama H.: Inconsistent relations among major ions and water stable isotopes in Antartica snow under different accumulation environments. Polar Science, 10, doi:10.1016/j.polar.2015.12.003, 2016.

Johnsen S. J.: Stable isotope homogenization of polar firn and ice, in Isotopes and Impurities in Snow and Ice, Proceeding of the Grenoble Symposium, August/September 1975, 210–219, IAHS AISH Publication, 118, Grenoble, France, 1997.

Johnsen S. J., Clausen H. B., Cuffey K. M., Hoffman G., Schwander J., and Creyts T.: Diffusion of stable isotopes in polar firn and ice: The isotope effect in firn diffusion, in Physics of Ice Core Records, edited by T. Hondoh, 121–140, Hokkaido University Press, Sapporo, Japan, 200.

564 Johnsen S. J., Dahl-Jensen D., Gundestrup N., Steffensen J. P., Clausen H. B., Miller
565 H., Masson-Delmotte V., Sveinbjörnsdottir A. E., and White J.: Oxygen isotope
566 and palaeotemperature records from six Greenland ice-core stations: Camp
567 Century, DYE-3, GRIP, GISP2, Renland and NorthGRIP, Journal of Quaternary
568 Science, 16, 299–307, doi:10.1002/jqs.622, 2001.
569 Jouzel J. and Merlivat L.: Deuterium and oxygen 18 in precipitation: Modeling of the
570 isotopic effects during snow formation, Journal of Geophysical Research, 89,
571 11749–11757, doi:10.1029/JD089iD07p11749, 1984.
572 Jouzel J., Merlivat L., Petit J. R., and Lorius C.: Climatic information over the last
573 century deduced from a detailed isotopic record in the South Pole snow, Journal of
574 Geophysical Research, 88, 2693–2703, doi:10.1029/JC088iC04p02693, 1983.
575 Jouzel J., et al.: Validity of the temperature reconstruction from water isotopes in ice
576 cores, Journal of Geophysical Research, 102, 26471–26487,
577 doi:10.1029/97JC01283, 1997.
578 Jouzel J., Vimeux F., Caillon N., Delaygue G., Hoffman G., Masson-Delmotte V., and
579 Parrenin F.: Magnitude of isotope/temperature scaling for interpretation of central
580 Antarctic ice cores, Journal of Geophysical Research, 108, 1–6,
581 doi:10.1029/2002JD002677, 2003.
582 Kaempfer T. U., and Schneebeli M. Observation of isothermal metamorphism of new
583 snow and interpretation as a sintering process, Journal of Geophysical Research,
584 112(D24), 1–10, doi:10.1029/2007JD009047, 2007.
585 Krinner G. and Werner M.: Impact of precipitation seasonality changes on isotopic
586 signals in polar ice cores: A multi-model analysis, Earth and Planetary Science
587 Letters, 216, 525–538, doi:10.1016/S0012-821X(03)00550-8, 2003.

588 Lorius C., Merlivat L., Jouzel J., and Pourchet M.: A 30,000-yr isotope climatic record
589 from Antarctica ice, Nature, 280, 644–648, doi:10.1038/280644a0, 1979.
590 Löwe H., Spiegel J. K., and Schneebeli M.: Interfacial and structural relaxations of
591 snow under isothermal conditions, Journal of Glaciology, 57, 499-510,
592 doi:10.3189/002214311796905569, 2011.
593 Masson-Delmotte V., Steen-Larsen H. C., Ortega P., Swingedouw D., Popp T., Vinther
594 B. M., Oerter H., Sveinbjornsdottir A. E., Gudlaugsdottir H., Box J. E., Falourd S.,
595 Fettweis X., Gallee H., Garnier E., Jouzel J., Landais A., Minster B., Paradis N.,
596 Orsi A., Risi C., Werner M., and White J. W. C.: Recent changes in north-west
597 Greenland climate documented by NEEM shallow ice core data and simulations,
598 and implications for past temperature reconstructions, The Cryosphere, 9, 1481-
599 1504, doi:10.5194/tc-9-1481-2015, 2015.
600 Merlivat L. and Jouzel J.: Global climatic interpretation of the deuterium-oxygen 18
601 relationship for precipitation, Journal of Geophysical Research, 84, 5029–5033,
602 doi:10.1029/JC084iC08p05029, 1979.
603 Neumann T. A.: Effects of firn ventilation on geochemistry of polar snow, PhD thesis,
604 University of Washington, Washington, USA, 2003.
605 Neumann T. A. and Waddington E. D.: Effects of firn ventilation on isotopic exchange,
606 Journal of Glaciology, 50, 183–194, 2004.
607 Neumann T. A., Albert M. R., Lomonaco R., Engel C., Courville Z., and Perron F.:
608 Experimental determination of snow sublimation rate and stable-isotopic exchange,
609 Annals of Glaciology, 49, 1–6, doi:10.3189/172756408787814825, 2008.
610 Otsu N.: A Threshold Selection Method from Gray-Level Histograms, IEEE
611 Transactions on Systems Man and Cybernetics, 9, 62–66, 1979.

612 Penna, D., Stenni, B., Šanda, M., Wrede, S., Bogaard, T. A., Michelini, M., et al.:
613 Technical Note: Evaluation of between-sample memory effects in the analysis of
614 δ2H and δ18O of water samples measured by laser spectroscopes. Hydrology and
615 Earth System Sciences, 16(10), 3925–3933. http://doi.org/10.5194/hess-16-3925-
616 2012, 2012.
617 Persson A., Langen P. L., Ditlevsen P., and Vinther B. M.: The influence of
618 precipitation weighting on interannual variability of stable water isotopes in
619 Greenland, Journal of Geophysical Research – Atmosphere, 116, 1-13,
620 doi:10.1029/2010JD015517, 2011.
621 Petit J. R., et al.: Climate and atmospheric history of the past 420,000 years from the
622 Vostok ice core, Antarctica, Nature, 399, 429–436, doi:10.1038/20859, 1999.
623 Pinzer B. R. and Schneebeli M.: Snow metamorphism under alternating temperature
624 gradients: Morphology and recrystallization in surface snow, Geophysical Research
625 Letters, 36, doi:10.1029/2009GL039618, 2009.
626 Pinzer B. R., Schneebeli M., and Kaempfer T. U.: Vapor flux and recrystallization
627 during dry snow metamorphism under a steady temperature gradient as observed by
628 time-lapse microtomography, The Cryosphere, 6, 1141–1155, doi:10.5194/tc-6-
629 1141-2012, 2012.
630 Ramseier R. O: Self-diffusion of tritium in natural and synthetic ice monocrystals,
631 Journal of Applied Physics, 38, 2553-2556, 1967.
632 Ritter F., Steen-Larsen H. C., Werner M., Masson-Delmotte V., Orsi A., Behrens M.,
633 Birnbaum G., Freitag J., Risi C., and Kipfstuhl S.: Isotopic exchange on the diurnal
634 scale between near-surface snow and lower atmospheric water vapor at Kohnen
635 station, East Antarctiva, The Cryosphere Discussion, doi:10.5194/tc-2016-4, in
636 review, 2016.

637 Schleef S., Jaggi M., Löwe H., and Schneebeli M.: Instruments and Methods: An
638 improved machine to produce nature-identical snow in the laboratory, Journal of
639 Glaciology, 60, 94–102, 2014.
640 Sjolte J., Hoffmann G., Johnsen S. J., Vinther B. M., Masson-Delmotte V., and Sturm
641 C.: Modeling the water isotopes in Greenland precipitation 1959-2001 with the
642 meso-scale model remo-iso, Journal of Geophysical Research, 116, 1-22,
643 doi:10.1029/2010JD015287, 2011.
644 Sokratov S. A. and Golubev V. N.: Snow isotopic content change by sublimation.
645 Journal of Glaciology, 55(193), 823-828, doi:10.3189/002214309790152456, 2009.
646 Steen-Larsen H. C., Masson-Delmotte V., Sjolte J., Johnsen S. J., Vinther B. M., Breon
647 F. M., Clausen H. B., Dahl-Jensen D., Falourd S., Fettweis X., Gallee H., Jouzel J.,
648 Kageyama M., Lerche H., Minster B., Picard G., Punge H. J., Risi C.,
649 Salas D., Schwander J., Steffen K., Sveinbjornsdottir A. E., Svensson A., and
650 White J.: Understanding the climatic signal in the water stable isotope records from
651 the neem shallow firn/ice cores in northwest Greenland, Journal of Geophysical
652 Research - Atmosphere, 116, 1–20, doi:10.1029/2010JD014311, 2011.
653 Steen-Larsen H. C., Johnsen S. J., Masson-Delmotte V., Stenni B., Risi C., Sodemann
654 H., Balslev-Clausen D., Blunier T., Dahl-Jensen D., Ellehøj M. D., Falourd S.,
655 Grindsted A., Gkinis V., Jouzel J., Popp T., Sheldon S., Simonsen S. B., Sjolte J.,
656 Steffensen J. P., Sperlich P., Sveinbjörnsdóttir A. E., Vinther B. M., and Whiste J.
657 W. C.: Continuous monitoring of summer surface water vapor isotopic composition
658 above the Greenland Ice Sheet, Atmospheric Chemistry and Physics, 13, 4815–
659 4828, doi: 10.5194/acp-13-4815-2013, 2013.
660 Steen-Larsen H. C., Masson-Delmotte V., Hirabayashi M., Winkler R., Satow K., Prié
661 F., Bayou N., Brun E., Cuffey K. M., Dahl-Jensen D., Dumont M., Guillevic M.,

662 Kipfstuhl S., Landais A., Popp T., Risi C., Steffen K., Stenni B., and
663 Sveinbjörnsdottir A. E.: What controls the isotopic composition of Greenland
664 surface snow?, Climate of the Past, 10, 377–392, doi:10.5194/cp-10-377-2014.,
665 2014a.
666 Steen-Larsen H. C., Sveinbjörnsdottir A. E., Peters A. J., Masson-Delmotte V.,
667 Guishard M. P., Hsiao G., Jouzel J., Noone D., Warren J. K., and White J. W. C.:
668 Climatic controls on water vapor deuterium excess in the marine boundary layer of
669 the North Atlantic based on 500 days of in situ, continuous measurements,
670 Atmospheric Chemistry and Physics, 14, 7741-7756, doi:10.5194/acp-14-7741-
671 2014., 2014b.
672 Sturm M. and Johnson J. B.: Natural convection in the subarctic snow cover, Journal of
673 Geophysical Research, 96, 11657–11671, doi:10.1029/91JB00895, 1991.
674 Town M. S., Warren S. G., Walden V. P., and Waddington E. D.: Effect of atmospheric
675 water vapor on modification of stable isotopes in near-surface snow on ice sheets,
676 Journal of Geophysical Research-Atmosphere, 113, 1-16,
677 doi:10.1029/2008JD009852, 2008.
678 Van der Wel G., Fischer H., Oerter H., Meyer H., and Meijer H. A. J.: Estimation and
679 calibration of the water isotope differential diffusion length in ice core records, The
680 Cryosphere Discussion, 9, 927-973, doi:10.5194/tc-9-1601-2015, 2015
681 Waddington E. D., Cunningham J., and Harder S. L.: The effects of snow ventilation on
682 chemical concentrations, in: Chemical Exchange Between the Atmosphere and
683 Polar Snow, edited by: Wolff, E. W. and Bales, R. C., Springer, Berlin, NATO ASI
684 Series, 43, 403–452, 1996.

685 Waddington E. D., Steig E. J., and Neumann T. A.: Using characteristic times to assess
686 whether stable isotopes in polar snow can be reversibly deposited. Annals of
687 Glaciology, 35, 118–124, doi:10.3189/172756402781817004, 2002.
688 Werner M., Langebroek P. M., Carlsen T., Herold M., and Lohmann G.: Stable water
689 isotopes in the ECHAM5 general circulation model: Toward high-resolution
690 isotope modeling on a global scale, Journal of Geophysical Research Atmosphere,
691 116, D15109, doi:10.1029/2011JD015681, 2011.
692 White J. W., Barlow L. K., Fisher D., Grootes P., Jouzel J., Johnsen S. J., Stuiver M.,
693 and Clausen H.: The climate signal in the stable isotopes of snow from Summit,
694 Greenland: Results of comparisons with modern climate observations, Journal of
695 Geophysical Research, 102, 26425–26439, doi:10.1029/97JC00162, 1997.
696 Zermatten E., Schneebeli M., Arakawa H., and Steinfeld A.: Tomography-based
697 determination of porosity, specific area and permeability of snow and comparison
698 with measurements, Cold Regions Science and Technology, 97, 33–40,
699 doi:10.1016/j.coldregions.2013.09.013, 2014.
700
701

Table 1: Morphological properties and flow characteristics of the experimental runs: μCT measured snow density (ρ), porosity (ε), specific surface area per unit mass (SSA), mean pore space diameter (d_{mean}), superficial velocity in snow (u_D), corresponding Reynolds number ($Re = d_{mean} \cdot u_D/\nu_{air}$), average inlet temperature of the humidifier and at the inlet ($T_{in,mean}$), average outlet temperature at the outlet ($T_{out,mean}$), and average temperature gradient (∇T_{ave}). Experiment (1) corresponds to the isothermal conditions; Experiment (2) to air warming; and Experiment (3) to air cooling in the snow sample.

	ρ kg m^{-3}	ε –	SSA m^2 kg^{-1}	d_{mean} mm	u_D m s^{-1}	Re –	$T_{in,mean}$ °C	$T_{out,mean}$ °C	∇T_{ave} K m^{-1}
Experiment (1)	202	0.78	28	0.39	0.03	0.76	-15.5	-15.5	–
Experiment (2)	202	0.78	30	0.36	0.03	0.70	-15.4	-14.0	+47
Experiment (3)	220	0.76	27	0.37	0.031	0.74	-12.3	-14.1	-60

711 **Table 2:** $\delta^{18}O$ in the vapor in the humidifier ($\delta^{18}O_{hum}$) and of the snow in the sample
712 holder ($\delta^{18}O_s$) at the beginning ($t = 0$) and end (t = end) of each experiment and the final
713 $\delta^{18}O$ content of the snow in the sample holder at the inlet ($z = 0$ mm) and outlet ($z = 30$
714 mm). Experiment (1) corresponds to the isothermal conditions; Experiment (2) to air
715 warming; and Experiment (3) to air cooling in the snow sample.
716

	$\delta^{18}O_{hum}$ ‰		$\delta^{18}O_{s,\ t=0}$ ‰	$\delta^{18}O_{s,\ t=end}$ ‰	
	$t = 0$	t = end		$z = 0$ mm	$z = 30$ mm
Experiment (1)	-68.2	-67.5	-10.97	-17.75	-15.72
Experiment (2)	-66.3	-66.1	-11.94	-19.60	-16.60
Experiment (3)	-62.8	-62.2	-10.44	-25.53	-15.00

717

Figure captions

Fig. 1. Schematic of the experimental setup. A thermocouple (TC) and a humidity sensor (HS) inside the humidifier measured the the mean temperature and humidity of the airflow. Two thermistors (NTC) close to the snow surface measured the inlet and outlet temperature of the airflow (Ebner et al., 2014). The Picarro Analyzer measured the isotopic composition $\delta^{18}O$ of the outlet flow. Inset: 3D structure of 110 × 42 × 110 voxels (2 × 0.75 × 2 mm^3) obtained by the μCT.

Fig. 2. Temporal isotopic composition of $\delta^{18}O$ of the outflow for each of the experimental runs. The spikes in the $\delta^{18}O$ were due to small temperature changes in the cold laboratory (Ebner et al., 2014). Exp. (1) corresponds to the isothermal conditions; Exp. (2) to air warming; and Exp. (3) to air cooling in the snow sample. The higher the recrystallization rate of the snow the slower the adaption of $\delta^{18}O$ of the outlet air to the inlet air. The illustration in the lower right corner shows the relation between $\delta^{18}O$ of the initial snow, inlet, and outlet of the air.

Fig. 3. Spatial isotopic composition of $\delta^{18}O$ of the snow sample at the beginning (t = 0) and at the end (t = end) for each experiment. The air entered at z = 0 mm and exited at z = 30 mm. Exp. (1) corresponds to the isothermal conditions; Exp. (2) to air warming; and Exp. (3) to air cooling in the snow sample.

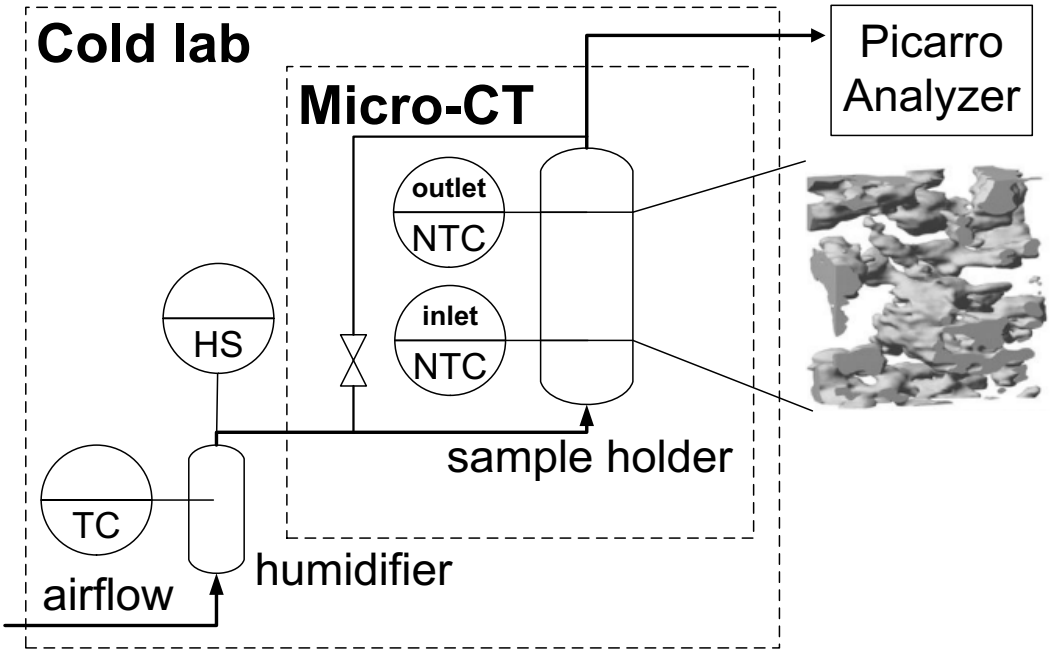
Cold lab
Micro-CT
Picarro
Analyzer
outlet
NTC
inlet
NTC
HS
sample holder
TC
humidifier
airflow

739

740 Fig. 1

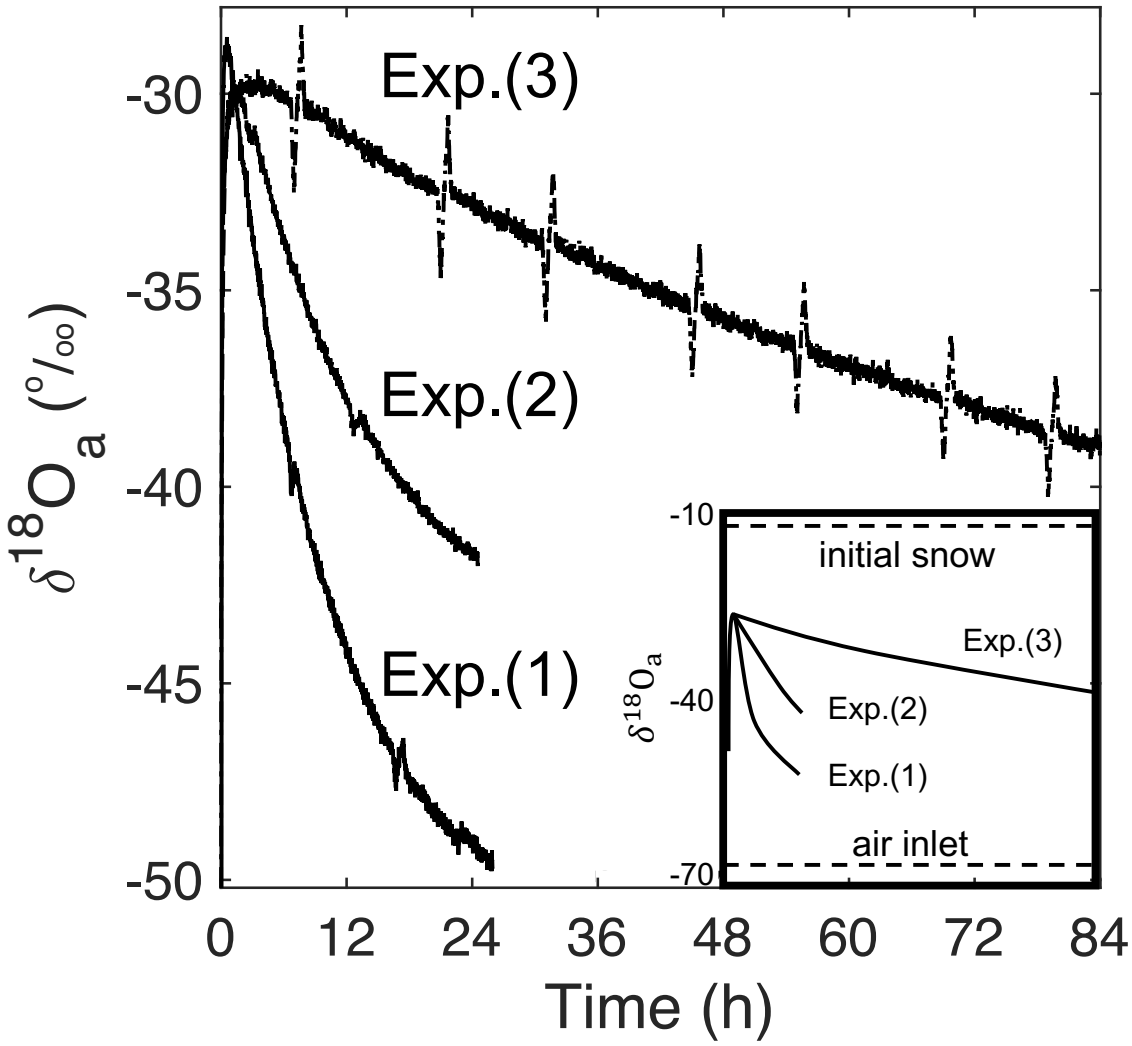

741

742 Fig. 2

743

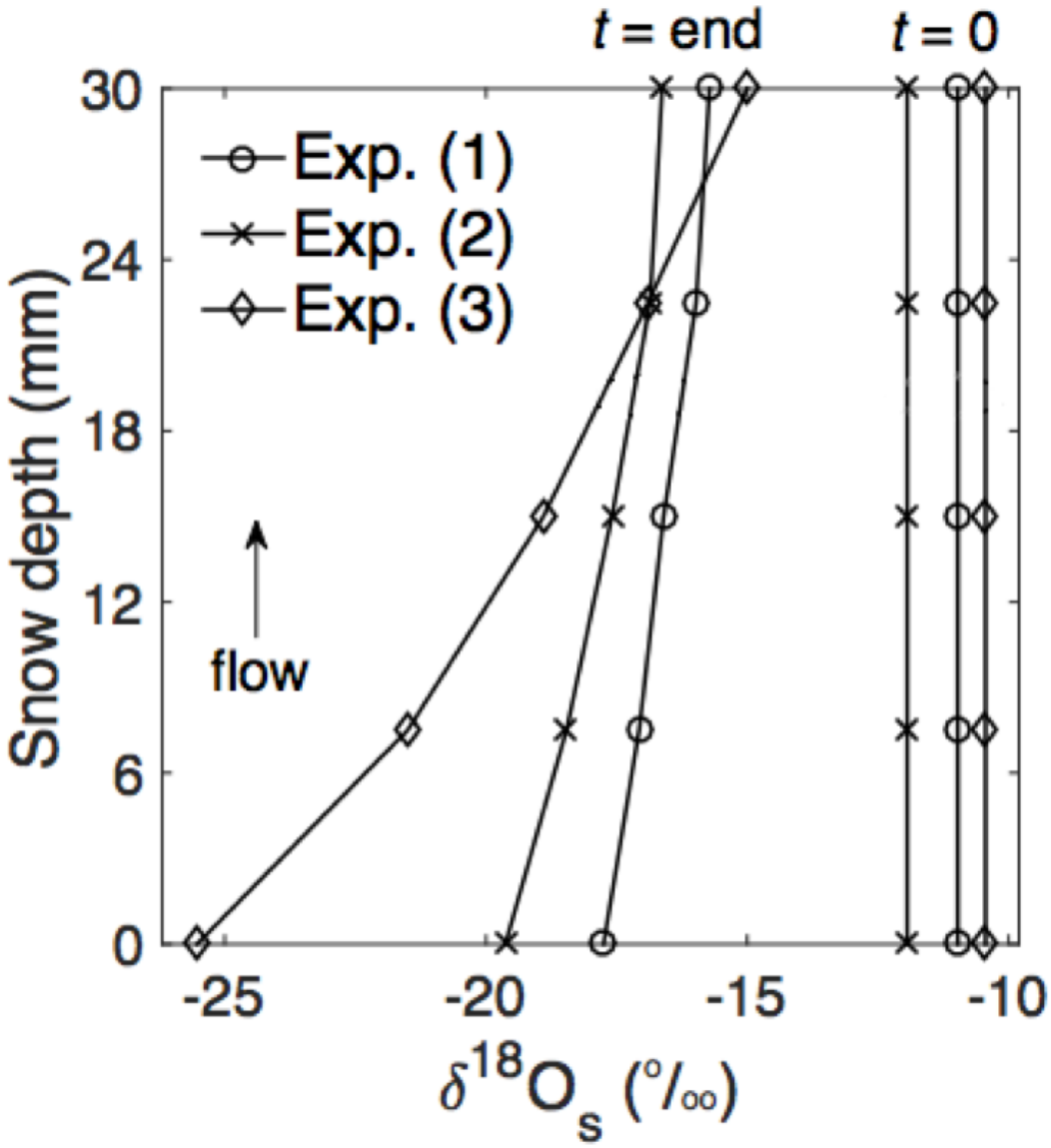
t = end
t = 0
30
24
18
12
6
0
Snow depth (mm)
Exp. (1)
Exp. (2)
Exp. (3)
flow
-25
-20
-15
-10
δ18Os (°/oo)

744

745 Fig. 3